JOURNAL OF CATALYSIS 37, 8–21 (1975)

Pulsed Thermo Kinetic (PTK) Measurements: Ethylene Hydrogenation

J. T. RICHARDSON AND H. FRIEDRICH

Department of Chemical Engineering, University of Houston, Houston, Texas 77004

Received August 24, 1973

Pulsed thermo kinetic (PTK) measurements have been applied to the study of hydrogen and ethylene adsorption on a nickel–alumina catalyst and of ethylene hydrogenation. A small fraction of the surface is covered by irreversible hydrogen with adsorption heats greater than 12 kcal/mole. There is a distribution of these heats up to 20 kcal/mole at 25°C but the distribution becomes more uniform with increasing temperature.

At 25°C, ethylene adsorbs on the bare nickel surface to cover 5% of the surface with a species showing a structure of C_2H_2 and an enthalpy of −5.87 kcal/mole. The same species is deposited at 150°C, mostly by self-hydrogenation to ethane and to the same extent, followed by the formation of a carbide or polymer. At 250°C, a parallel reaction results in the formation of methane and a highly hydrogen deficient residue. All measured heats are in close agreement with those calculated from theoretical models.

With preadsorbed hydrogen, the same reactions occur but only after the hydrogen has been removed by a much faster reaction with molecular or adsorbed ethylene.

Ethylene, pulsed into flowing hydrogen, reacts to ethane with an exothermic heat at 25°C and an endothermic heat above 25°C. It is postulated that weakly π-adsorbed ethylene reacts with strongly held hydrogen atoms in the interstices of the (100) plane and that the rate of formation of these adatoms is rate limiting. At high temperature, methane is formed by reaction with more accessible hydrogen.

INTRODUCTION

Ethylene hydrogenation and the associated adsorption of ethylene and hydrogen are among the most widely studied processes in catalysis research (*1*). There is still some uncertainty, however, regarding the modes of adsorption of both hydrogen and ethylene and of the mechanisms for ethylene hydrogenation (*2*). Accordingly, we have selected this reaction as an example of the applicability of pulsed thermo kinetics (PTK) studies (*3*) to surface mechanisms. In fact, it was the completely unexpected results obtained during attempts to calibrate the PTK method with ethylene hydrogenation that led us to appreciate the potential of these measurements in separating adsorption and reaction steps in catalytic reactions.

Practically every conceivable reaction path has been suggested for ethylene hydrogenation (*1,2,4–8*). It is clear that the mechanism is not simple and may indeed involve several competing paths acting under different conditions. A reaction between surface species involving a "half-hydrogenated" state has been widely discussed (*6*). The possibilities of reactions between molecular ethylene (*7*) or hydrogen (*8*) and the other adsorbed species have also been introduced. Attempts to explain a maximum in the rate of ethylene hydrogenation over nickel at about 150°C have led to a mechanism suggesting different adsorptive approximations in a surface-type reaction, although a change in path must not be ruled out (*10*).

The key to an understanding of the sur-

face mechanisms is a knowledge of the modes of adsorption of ethylene and hydrogen. Both structure and reactivity are important.

Ethylene may adsorb in many forms—π and σ bonding (*11*), single or dual site, associated or dissociated (*1*). Theoretical calculations of adsorption heats have been made (*1*) but very little experimental verification published. Evidence for all types of adsorption have been advanced with the results seemingly dependent on the conditions of the experiment (*12–14*).

Hydrogen is just as complicated. Several types of adsorbed hydrogen are possible (*5*). Theoretical models and calculations suggest widely different heats of adsorption for structure sensitive sites (*15*). The arguments of whether the distribution of heats means a priori or induced heterogeneity still continue (*16*).

What then are the reaction paths and which types of adsorbed species are involved? Pulsed thermo kinetic measurements offer a partial answer to these questions. Perhaps, together with other physical methods, these will lead to a greater understanding of this seemingly simple system.

EXPERIMENTAL

The general principles, design and techniques of the PTK method have been described in a previous article (*3*). Measurements were obtained in the apparatus shown in Figs. 1 and 2 of that article. All precautions and corrections necessary to calibrate and interpret the results were carried out.

The catalyst used was a nominal 50% NiO/Al_2O_3 prepared by co-precipitation from mixed nitrate solutions. After washing, the catalyst was heat-treated at 500°C in flowing air and then reduced in hydrogen for 16 hr at 375°C. After stabilization with small amounts of oxygen, the catalyst was charged to the cell of the PTK or any other apparatus and completely reduced with hydrogen at 375°C for three hours without excessive shrinkage or water formation.

The extent of nickel reduction and dispersion were determined by auxilliary magnetic susceptibility and hydrogen surface area measurements. For magnetic data we used a conventional Faraday apparatus consisting of an Alfa Model 4800 electromagnet and a Cahn RG microbalance. The sample was reduced at 375°C prior to the measurement of magnetization versus magnetic field at 25°C. These data are shown in Fig. 1. The catalyst was then sintered in helium at 600°C in order to yield sufficiently large crystallites so that magnetic saturation could be achieved. From these results, the amount of reduced nickel in the catalyst was found to be 39.5%. The initial slope of Fig. 1 was used to calculate a low field volume average (*5*) of 2.20×10^5 Å^3.

Hydrogen chemisorption data were measured with a standard volumetric adsorption apparatus. The resulting isotherm, shown in Fig. 2, exhibits an initial large and irreversible adsorption followed by a

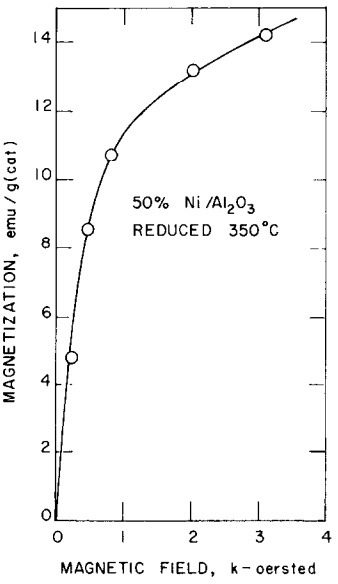

FIG. 1. Magnetization data at 25°C for the reduced $Ni–Al_2O_3$ catalyst.

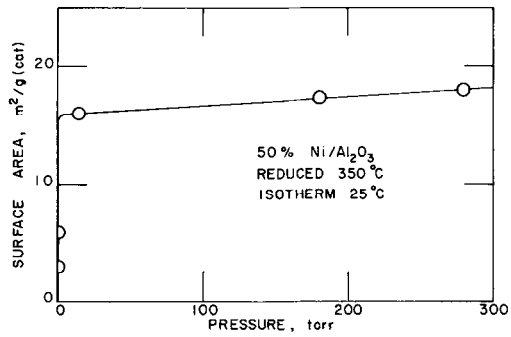

FIG. 2. Hydrogen adsorption isotherm at 25°C for the reduced $Ni-Al_2O_3$ catalyst.

slow increase as the pressure increases. If we make the assumption that the irreversible adsorption corresponds to monolayer coverage, the resulting surface area is 14.5 m^2/g (cat).

The volume determined from magnetic measurements may be used to calculate a surface area if the shape of the crystallites is known. For spheres the diameter of the crystallite would be 75 Å, with a surface area of 35.5 m^2/g (cat). The discrepancy with the measured value is much too large to be experimental error and the temperature of reduction too low for "skin" effects (*17*). However, if the calculation is made assuming hemispheres, the diameter and surface area are 94 Å and 14.1 m^2/g (cat), respectively. The very good agreement between this model and experiment supports the arguments (*18*) that the nickel crystallites are indeed hemispheres, supported in this case on Al_2O_3 or $NiAl_2O_4$ (*19*).

The sample charge to the PTK cell was 0.2 g of catalyst mixed with 0.6 g of α-Al_2O_3, both crushed to approximately 300 μm size. The reference sample was α-Al_2O_3. Chromel-alumel thermocouples were used in the differential temperature measurement.

The sample was heated at 10°C/min in a stream of hydrogen to 375°C and held at this temperature for 3 hr. Following reduction the nickel surface was cleaned with a 30 min treatment in helium at 400°C. This procedure was sufficient since subsequent pulsing with ethylene at 25°C did not result in ethane formation, indicating the absence of adsorbed hydrogen on the nickel surface. A calibrated loop of approximately 6×10^{-6} g moles of gas was used to pulse both hydrogen and ethylene. The carrier helium or hydrogen gas flow rate was maintained at 10 cm^3/min. The composition of the effluent peak was determined using a 12 in., 0.25 in. o.d. column of 60–100 mesh activated silica gel and a Gow-Mac Model 10-133 Thermistor Cell.

For adsorption measurements the pulse size was large enough that zoning did not occur, i.e., breakthrough or near breakthrough took place in the first pulse. For the ethylene hydrogenation measurements, however, there were strong indications that zoning was involved. Accordingly, it was necessary to calibrate with this in mind, using the procedures outlined in the previous article (*3*) to determine both an overall and a length-dependent calibration factor. This was accomplished with both ethylene hydrogenation and oxygen adsorption at 25°C.

Three series of experiments were conducted, with a fresh sample for each experiment: (1) adsorption of ethylene (helium carrier) at 25°C, 150°C and 250°C; (2) adsorption of hydrogen, followed by adsorption of ethylene at 25°C, 150°C and 250°C; (3) reaction of ethylene in hydrogen at 25°C, 150°C and 250°C.

RESULTS AND DISCUSSION

Although we conducted the experiments in the order outlined above, it is more instructive to discuss them in the sequence (1) hydrogen adsorption, (2) ethylene adsorption, (3) ethylene reaction with preadsorbed hydrogen, and (4) ethylene reaction in hydrogen.

1. Hydrogen Adsorption

The results of pulsing hydrogen at 25°C are given in Table 1. The initial pulse was

TABLE 1
H_2 ON CLEAN NICKEL AT 25°C[a]

Pulse no.	Observed heats (calories × 10^6) exo	endo	Effluent (g moles × 10^6) H_2	H_2 retained (g moles × 10^6)
1	8.99	—	0.58	5.27
2	2.66	0.68	4.29	1.56
3	2.28	1.02	4.88	0.97
4	1.95	1.19	5.27	0.58
5	1.82	1.54	5.60	0.25
6	1.65	1.65	5.85	—
7	1.65	1.65	5.86	—

[a] Pulse size: 5.85 × 10^{-6} g moles.

almost entirely irreversibly adsorbed. This form of adsorption has an associated exothermic heat. With each successive pulse, the amount of irreversible adsorption was less, ceasing with pulse number 6. The total amount retained corresponds to only about 0.2 of the full monolayer coverage calculated from the adsorption isotherm in Fig. 2.

As the amount of irreversible adsorption in each pulse decreased, the exothermic peak also decreased and an increasingly endothermic peak appeared. Finally, after the sixth pulse, the amounts of exo- and endothermic heat were equal, indicating that reversible adsorption and desorption had taken place in the pulse. The shapes of these peaks are shown in Fig. 3. The endothermic or desorption step is sufficiently slow that the adsorption–desorption parts may be fairly accurately resolved. Thus, in pulse number 2 for example, the difference between the exothermic and endothermic peak has been taken as the heat of adsorption of the irreversibly adsorbed hydrogen.

In this way the histogram in Fig. 4 was calculated. The dotted curve represents the decrease of the heat of adsorption with coverage. Attempts to refine the histogram by pulsing smaller doses of hydrogen were attempted. Serious zoning was encountered with the apparatus then in use. The accuracy was not sufficiently improved over that in Fig. 4 to warrant further investigation.

Results at higher temperatures (150°C, 250°C) followed essentially the same trend, with the following comparisons: (1) the total amount of irreversible adsorption remained approximately the same (0.2 of full coverage); (2) the fractions of hydrogen irreversibly adsorbed in the first pulse for 25, 150, and 250°C were 0.9, 1.0 and 0.5, respectively; (3) with increasing temperatures, the amount retained in each pulse became proportional to the time between pulses, indicating desorption of the adsorbed hydrogen. Only by rapid pulsing was it possible to achieve consistent results; (4) the heat of adsorption

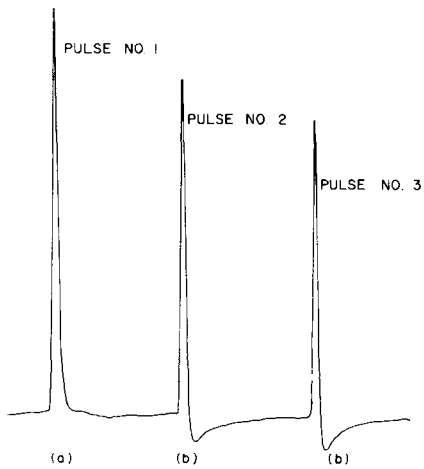

FIG. 3. Pulsed thermo kinetic (PTK) peaks of hydrogen adsorption: (a) irreversible adsorption, (b) reversible adsorption.

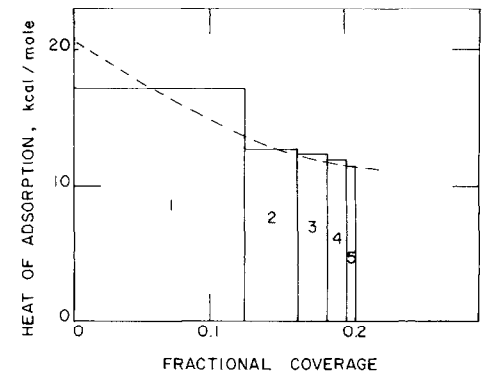

FIG. 4. Enthalpies of adsorption of hydrogen pulses at 25°C.

versus coverage curves changed with increasing temperature, as shown in Fig. 5.

The curve for 25°C shown in Fig. 5 is generally consistent with earlier results using more conventional techniques (*20*). However, the initial heat for zero coverage is lower than the usually observed value of 30 kcal/mole. Distribution in adsorption heat with coverage is usually attributed to a priori heterogeneity, although arguments for induced effects still persist (*16*). The possible existence of different types of adsorption sites at various crystal faces and in dislocations or imperfections must be acknowledged. Indeed, the localized bond theory of adsorption provides further evidence for surface heterogeneity through different surface orbital symmetries existing on different faces (*21*). Quantum mechanical calculations have shown how these may lead to a distribution in heats (*15*). However, if we rule out support poisoning effects, the only way to reconcile site heterogeneity with the temperature dependence shown in Fig. 5 is to assume an approach to homogeneity with increasing temperature. Such a phenomenon could result from either a change in the surface mobility or a change in the nature of the sites. If adsorption takes place on the weaker sites and is followed by migration to the stronger sites, then the low initial heat observed for the pulse could be attributed to slow migration within the time scale of the pulse. A decrease in mobility at higher temperatures would then lead to additional lowering over the initial heats. Further indications of this model are given by the experiments on ethylene hydrogenation discussed in a later section.

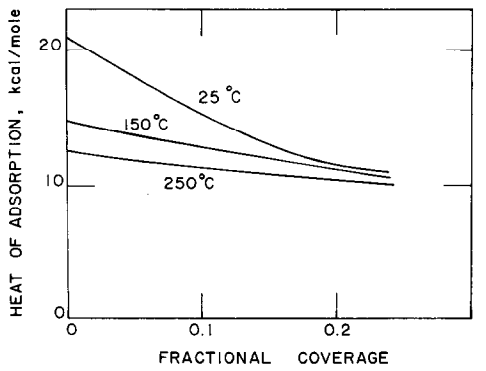

FIG. 5. Distribution of adsorption enthalpies for hydrogen adsorption at 25, 150, and 250°C.

Changes in the nature of the sites is a possibility. However, the ethylene hydrogenation results show conclusively that high energy sites exist, at least at high hydrogen coverage. We must, therefore, consider surface migration as the most reasonable explanation.

The cut off point between irreversible and reversible adsorption remains the same, 10–12 kcal/mole. This is consistent with earlier results which give values of 10 kcal/mole for reversible heats (*22,23*).

We shall now speculate further on the reasons for the low coverage (0.22 of a monolayer) at 25°C. It has been postulated that the shapes of supported nickel crystallites are face-centered cubic cubo-octahedra (*24*), or in our case, semi-cubo-octahedra. For perfect cubo-octahedra, only (100) and (111) faces are present. We have calculated the relative number of atoms on these faces for a perfect cubo-octahedron of the size measured for our sample. The fraction of surface atoms on the (100) face is 0.23. Such close agreement with experimental results leads us to the hypothesis that irreversible adsorption occurs on (100) atoms only. This viewpoint is consistent with the model calculations of adsorption heats (*15*) which show that only (100) atoms have values greater than 10 kcal/mole. For imperfect cubo-octahedra, small fractions of (110) atoms are present.

We made no attempt to interpret the heats associated with the reversible adsorption. This would require a knowledge of the total number of adsorption–desorption steps. Such information is obtainable,

at least in theory, from the shape of the effluent peak (*24,25*).

2. Ethylene Adsorption

Possible modes of ethylene adsorption on nickel have been reviewed by Eley (*1*) and are given in Table 2, together with his calculation of the associated heats. Also given in Table 2 is the reaction for carburization, with the heat calculated from the data of Browning and Emmett (*26*).

It is generally accepted on the basis of infrared and kinetic evidence (*6*) that ethylene adsorbed on clean nickel surfaces at 25°C results in dissociated species, probably represented by reactions (4) and (6) in Table 2. Beeck concludes that it must be reaction (4) since no hydrogen appears in the gas phase when ethylene reacts with nickel films (*27*). However, magnetic measurements (*5*) show the involvement of only two nickel atoms rather than four as required by reaction (*4*). This suggests reaction (1), the associative form of adsorption, although reaction (6) is just as likely if hydrogen is not retained.

Our PTK results for ethylene on clean nickel at 25°C are given in Table 3. Each pulse resulted in a decreasing amount of irreversibly adsorbed ethylene. For each mole of ethylene adsorbed, approximately one mole of hydrogen was also detected in the effluent, a surprising result in contrast to Beeck's observations (*27*). However, this may reflect only the difference between a pulse and static experiment. The endothermic heat peak suggests that desorption occured. This may have been either desorption of the hydrogen from the dissociated ethylene molecule or reversibly adsorbed ethylene. The fact that the endothermic peak increased to a steady state while the hydrogen decreased with each pulse strongly suggests the reversibly adsorbed ethylene. This means that the hydrogen is released into the gas phase directly from the dissociating ethylene molecule and is not re-adsorbed irreversibly since all available sites are occupied. Perhaps if the hydrogen were not swept away in the pulse it too would be adsorbed initially.

We conclude from the stoichiometry that the adsorbed complex has the structure C_2H_2. Assuming that the difference between the exo- and endothermic peaks is the heat associated with this complex, the enthalpy of reaction is −5.87 kcal/mole.

TABLE 2
SUGGESTED MODELS AND ESTIMATED HEATS FOR ETHYLENE CHEMISORPTION ON NICKEL

Model	Heats of adsorption (kcal/mole)	
	Calculated	Observed
(1) $C_2H_4 + 2Ni \rightarrow Ni\diagup\!\!\diagdown\begin{matrix}CH_2—CH_2\end{matrix}\diagup\!\!\diagdown Ni$	−34	
(2) $C_2H_4 + Ni \rightarrow Ni—CH = CH_2 + \frac{1}{2}H_2$	−3	−3.17
(3) $C_2H_4 + Ni \rightarrow Ni = CH—CH_3$	−26	
(4) $C_2H_4 + 4Ni \rightarrow Ni\diagup\!\!\diagdown\begin{matrix}CH = CH\end{matrix}\diagup\!\!\diagdown Ni + 2NiH$	−23	
(5) $2C_2H_4 + 2Ni \rightarrow Ni\diagup\!\!\diagdown\begin{matrix}CH = CH\end{matrix}\diagup\!\!\diagdown Ni + C_2H_6$	−17	−16.2
(6) $C_2H_4 + 2Ni \rightarrow Ni\diagup\!\!\diagdown\begin{matrix}CH = CH\end{matrix}\diagup\!\!\diagdown Ni + H_2$	−6	−5.87
(7) $C_2H_4 + 6Ni \rightarrow 2Ni_3C + 2H_2$	+56.2	
(8) $C_2H_4 + 10Ni \rightarrow 2Ni_3C + 4NiH$	+32.2	+50.5

TABLE 3
C_2H_4 ON CLEAN NICKEL AT 25°C[a]

Pulse no.	Observed heats (calories × 10^2)		Effluent (g moles × 10^6)				C_2H_4 retained (g moles × 10^6)
	exo	endo	H_2	CH_4	C_2H_6	C_2H_4	
1	2.13	1.50	0.98	—	—	4.82	1.03
2	1.96	1.62	0.58	—	—	5.27	0.58
3	2.00	1.80	0.39	—	—	5.48	0.37
4	1.92	1.84	0.19	—	—	5.68	0.17
5	1.84	1.84	—	—	—	5.85	—

[a] Pulse size: 5.85 × 10^{-6} g moles.

This is remarkably close to the value of −6 kcal/mole calculated by Eley for reaction (6). The agreement supports not only Eley's calculation but also the structure assignment of a dissociatively adsorbed complex.

The amount of ethylene molecules irreversibly adsorbed was only 25% of the number of hydrogen molecules. Geometric and surface orbital considerations favor strong bonds on the (100) planes (*21*) so that ethylene adsorption most likely occurs on the same types of sites as hydrogen adsorption. However, only a fraction of the sites activate the dissociated species.

It is much more difficult to interpret the reversible heat. If we assume that each mole of ethylene was reversibly adsorbed only once as the pulse passed through the bed, the average enthalpy adsorption is −3.17 kcal/mole or close to that calculated for reaction (2). On this basis, it is tempting to associate the reversible adsorption with the single point dissociative adsorption.

Results for the experiments at 150°C are given in Table 4. The effluent data show the formation of ethane presumably by reaction (5). However, only about two thirds of the ethane in the first pulse was

TABLE 4
C_2H_4 ON CLEAN NICKEL AT 150°C[a]

Pulse no.	Observed heats (calories × 10^2)		Effluent (g moles × 10^6)				C_2H_4 retained (g moles × 10^6)
	exo	endo	H_2	CH_4	C_2H_6	C_2H_4	
1	2.65	—	tr	tr	0.66	4.21	0.98
2	1.42	0.34	tr	tr	0.47	4.60	0.77
3	0.59	0.38	tr	tr	0.34	4.90	0.61
4	0.20	0.40	—	—	0.28	5.04	0.53
5	—	0.58	—	—	0.17	5.24	0.48
6	—	0.69	—	—	0.14	5.32	0.39
7	—	0.75	—	—	0.08	5.46	0.31
8	—	0.86	—	—	0.05	5.58	0.27
9	—	0.93	—	—	0.04	5.58	0.27
10	—	0.93	—	—	0.02	5.60	0.23
11	—	0.98	—	—	tr	5.63	0.22
12	—	1.11	—	—	—	5.63	0.22

[a] Pulse Size: 5.85 × 10^{-6} g moles.

converted by this path. Only trace amounts of hydrogen were formed, so the remainder of the ethylene was retained through reactions (1), (3), or (4). The amount of self hydrogenation decreased with each pulse and the amount of retained ethylene per pulse reached a steady state.

The total number of ethane molecules converted by self-hydrogenation equaled the number of C_2H_2 species formed at 25°C. It follows that the same sites must be involved. At the lower temperature, hydrogen detaches itself from the adsorbing molecule directly into the gas phase. Re-adsorption under static conditions or removal in the transient pulse may then occur. The intermediate adsorbed species may be the associated complex. At higher temperatures ethylene from the gas phase reacts with this complex and carries off the hydrogen as ethane. In both cases, reaction ceases when the sites are filled with the C_2H_2 residue. The reaction responsible for the remainder of the conversion must take place on different sites.

The thermal peaks reveal a series of complex interactions. The shapes of these peaks are shown in Fig. 6. The first peak was exothermic and may very well represent a combination of reactions (1), (3), (4), and (5). The overall value for the enthalpy of reaction is −16.2 kcal/mole. This is indeed close to that calculated for reaction (5) but it is impossible to estimate further among the various potential reactions.

An endothermic peak appeared in the second pulse and grew progressively larger until it was the only effect. This is not the heat of desorption associated with a reversible mode since no corresponding exothermic adsorption occurred. It may represent the carburization reaction (8) since no hydrogen was liberated. By combining the calculated enthalpy value for reaction (7) with our lowest number for the heat of irreversible adsorption of hydrogen, we estimate a value of +32.2 kcal/mole for reaction (8). The measured

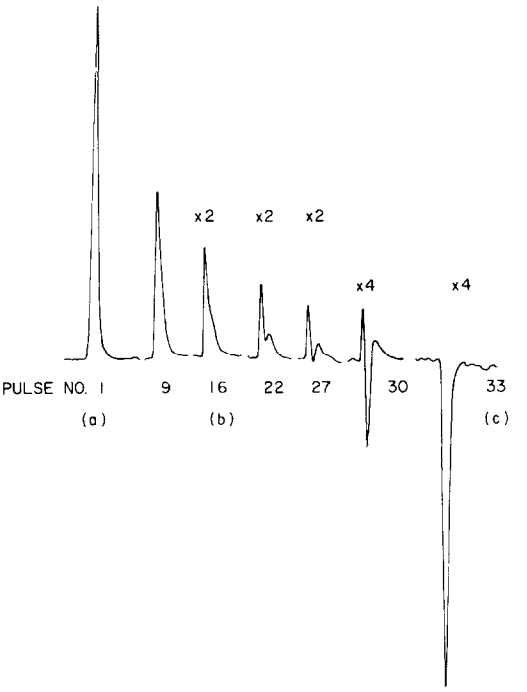

FIG. 6. PTK peaks for ethylene adsorption at 150°C: (a) reaction to form ethane, (b) beginning of carbonization or polymerization, (c) no hydrogenation but continued carbonization or polymerization.

value from pulse number 12 is +50.5 kcal/mole.

The most puzzling aspect of this interpretation is the absence of hydrogen in the effluent. Another possibility suggests itself. If indeed the ethylene not involved in self-hydrogenation is adsorbed with the hydrogen intact, the appearance of the endothermic peak may indicate further reaction with molecular ethylene to give a dimer of adsorbed butene. This path has been discussed previously (*28*). The associated heats for this reaction do indeed appear to be large, but not too large if we consider that butane or butene is not observed in the gas phase.

Results of the pulsing at 250°C are given in Table 5. Most of the first pulse was retained with a structure of approximately C_2H_2 but the evolved product was methane. The enthalpy of formation of the residue is found from the heat balance to

TABLE 5
C_2H_4 ON CLEAN NICKEL AT 250°C[a]

Pulse no.	Observed heats (calories × 10^{-2})		Effluent (g moles × 10^6)				C_2H_4 retained (g moles × 10^6)	
	exo	endo	H_2	CH_4	C_2H_6	C_2H_4	amount	H/C
1	10.25	—	0.39	3.06	0.08	—	4.24	1.17
2	3.59	1.47	0.19	4.89	0.18	—	3.17	0.38
3	3.22	0.99	tr	5.11	0.12	—	3.17	0.35
4	3.22	0.61	—	4.87	0.36	—	3.05	0.29
5	3.11	0.48	—	4.96	0.26	—	3.11	0.32
6	3.16	0.37	—	4.71	0.53	—	2.96	0.23
7	3.28	0.31	—	4.66	0.57	—	2.95	0.23
8	3.34	0.24	—	4.59	0.63	—	2.92	0.22
9	3.46	0.15	—	4.48	0.71	—	2.90	0.21
10	3.71	—	—	4.43	0.77	—	2.86	0.19
13	4.57	—	—	4.31	0.90	—	2.79	0.14
23	5.60	—	—	4.12	1.18	—	2.66	0.03
37	5.92	—	—	4.17	1.06	—	2.70	0.07

[a] Pulse Size: 5.85×10^{-6} g moles.

be +5.46 kcal/mole, in agreement with that from reaction (6).

After this first pulse, the behavior became more complex. First, the amount of methane increased and then decreased while the ethane steadily increased. Secondly, the residue became increasingly hydrogen deficient. An endothermic peak appeared in the second pulse but decreased subsequently until it was absent in the tenth pulse. This endothermic peak was not characteristic of a surface reaction but had the long tailing peak of slow desorption. The exothermic part decreased to a minimum at the fifth pulse and then increased again.

In attempting to explain this behavior, we are impressed by the simultaneous appearance of the endothermic peak and the hydrogen deficient residue. Apparently the products, or one of them, is more strongly held by this residue than by the clean nickel surface. Since the endothermic peak decreases as the ethane increases, we conclude that this is the product involved. The increased "coking" of the surface by the residue must result in less tightly held ethane, either because of polymerization or blocking. Desorption of the ethane is increased.

Final pulses deposited almost pure carbon. There is no question that this is not nickel carbide since there is no associated endothermic peak. It is not clear whether the methane originates from ethane hydrogenolysis via adsorbed hydrogen or from a parallel reaction yielding methane and the hydrogen deficient residue directly.

3. *Ethylene Reaction with Pre-adsorbed Hydrogen*

These experiments were carried out by pulsing ethylene over the same catalyst that had been treated with hydrogen during the hydrogen adsorption study. The reactions are between ethylene and the adsorbed hydrogen still on the surface.

At 25°C most of the hydrogen was retained. Results of the PTK measurements are given in Table 6. Ethylene reacted so rapidly that zoning occurred with breakthrough at the third pulse. The reactions were almost complete at this point, so that these three peaks are the most revealing.

TABLE 6
C_2H_4 ON PREADSORBED H_2 AT 25°C[a]

Pulse no.	Observed heats (calories × 10^2)		Effluent (g moles × 10^6)				C_2H_4 retained (g moles × 10^6)
	exo	endo	H_2	CH_4	C_2H_6	C_2H_4	
1	6.85	—	0.20	0.03	4.67	—	1.16
2	7.10	—	0.20	0.02	4.42	—	1.42
3	6.99	—	0.20	—	3.52	0.64	1.69
4	2.20	0.93	0.20	—	0.27	5.24	0.34
5	1.77	1.22	—	—	0.08	5.75	0.02
6	1.73	1.27	—	—	0.04	5.80	0.01
7	1.73	1.27	—	—	0.02	5.80	0.03

[a] Pulse Size: 5.85×10^{-6} g moles.

Reaction heats were exothermic, with the formation of ethane and an ethylene residue. Some free hydrogen was also evolved together with traces of methane. It seems most likely from the earlier results that the residue is C_2H_2. Indeed, in the first three pulses, the hydrogen requirements for the products are almost exactly met from the amount of preadsorbed hydrogen plus that stripped from C_2H_4. The dominant processes are therefore dissociative adsorption of C_2H_4 to C_2H_2 and the reaction between ethylene and adsorbed hydrogen. The last reaction is very fast and it is reasonable to conclude that the adsorbed hydrogen reacts with molecular or weakly adsorbed ethylene, although there is no direct evidence to rule out reactions between adsorbed species.

By correcting for the heat associated with the adsorption of the C_2H_2 complex, we calculated the enthalpy of the adsorbed hydrogen reacting with the ethylene. The results for pulses 1, 2, and 3 are −19.5, −18.6, and −15.7 kcal/mole, respectively. The average, −17.9 kcal/mole, is in approximate agreement with Fig. 4.

After the third pulse, the process was close to self-hydrogenation, but only in small quantities. All activity ceased when 4.67×10^{-6} moles of C_2H_2 had been adsorbed. This is approximately twice that retained in the absence of pre-adsorbed hydrogen. Others have also noted that preadsorption of hydrogen facilitates the adsorption of ethylene (5).

At 150°C, the results, shown in Table 7 are similar to those at 25°C, with the exception that the amount of C_2H_2 complex in each pulse increased. This higher activity for residue formation increased the number of pulses for breakthrough to seven. At this point, the preadsorbed hydrogen had been consumed. The average enthalpy of this adsorbed hydrogen was −12.5 kcal/mole. After the seventh pulse, the behavior closely followed that in Table 4, with the same endothermic peak.

Table 8 gives the results at 250°C. Several important differences are noted when these are compared to Table 5. While the amount of methane was approximately the same as before, the ethane fraction increased at the expense of the ethylene residue. It seems probable that the methane does not result from adsorbed hydrogen, but from a parallel reaction with C–C bond rupture of the ethylene. In order to satisfy hydrogen requirements the residue must be close to pure carbon. As with no adsorbed hydrogen, the endothermic peak originated from the desorption of the ethane. It decreased as the amount of coke increased.

The experiment was terminated after the ninth pulse and the surface dosed with

TABLE 7
C_2H_4 ON PREADSORBED H_2 AT 150°C[a]

Pulse no.	Observed heats (calories × 10^2) exo	endo	Effluent (g moles × 10^6) H_2	CH_4	C_2H_6	C_2H_4	C_2H_4 retained (g moles × 10^6)
1	5.41	—	0.29	0.07	3.85	—	1.96
5	8.89	—	0.10	0.04	3.47	—	2.36
7	6.44	—	tr	0.03	3.84	0.89	2.11
10	2.13	—	tr	0.01	1.31	3.77	0.76
18	1.18	—	—	—	0.71	4.64	0.50
30	.93	.32	—	—	0.43	5.20	0.22
40	—	1.06	—	—	—	5.63	0.22

[a] Pulse Size: 5.85 × 10^{-6} g moles.

TABLE 8
C_2H_4 ON PREADSORBED H_2 AT 250°C[a]

	Pulse no.	Observed heat (calories × 10^2) exo	endo	Effluent (g moles × 10^6) H_2	CH_4	C_2H_6	C_2H_4	C_2H_4/H_2 retained (g moles × 10^6)
	1	6.47	2.13	—	3.66	1.19	—	2.83
	2	5.13	1.07	tr	4.95	1.23	—	2.14
	3	5.45	0.64	tr	5.23	1.28	—	1.95
	4	5.83	0.75	tr	5.02	1.48	—	1.86
	5	6.15	0.30	tr	4.81	1.50	—	1.91
	6	6.42	0.11	tr	4.86	1.54	—	1.88
	9	7.05	0.53	tr	4.45	1.74	—	1.88
H_2								
	1	4.99	—	—	2.41	—	—	1.03
	2	5.31	1.17	1.14	1.87	—	—	0.97
	3	4.89	1.49	1.75	1.49	—	—	1.12
	4	4.57	1.70	2.15	1.22	—	—	1.26
	5	4.57	1.81	2.53	0.97	—	—	1.38
	6	4.68	1.70	2.73	0.80	—	—	1.52
	17	4.67	2.18	4.68	0.38	—	—	0.61
	25	4.89	2.76	5.46	0.15	—	—	0.09

[a] Pulse Size: 5.85 × 10^{-6} g moles.

hydrogen. The carbon was stripped as methane, the activity decreasing with each pulse. Some hydrogen was retained irreversibly. After correction for the heat of adsorption of this hydrogen, the heat of reaction of the stripping was calculated to be −15.8 kcal/mole CH_4. This is constant with each pulse, giving an enthalpy for the carbon of −3.80 kcal/mole.

In each of the experiments with pre-adsorbed hydrogen, the only major difference between those with no hydrogen adsorption was the initial fast formation of ethane. The reaction is most likely between molecular ethylene and the adsorbed hydrogen, although PTK results do not rule out surface reactions.

After the pre-adsorbed hydrogen is depleted the behavior is much the same as on the clean surface. It would appear, how-

ever, that the reaction between molecular ethylene and adsorbed hydrogen is much faster than the self-hydrogenation.

4. Ethylene Hydrogenation in Flowing Hydrogen

Pulsed thermo kinetic results for pulsed ethylene in hydrogen are given in Table 9. In all cases hydrogenation to ethane or methane was complete, with the amount of methane increasing with temperature. The concentration data do not show any surprises but the thermal data reveal most interesting and unexpected results. At 25°C the peaks were exothermic but at 150°C they were endothermic. With further increase in temperature, an exothermic peak appeared *after* the endothermic one, this second peak increasing with methane content in the product. Finally, the initial (and only) peak was again exothermic.

From these data we calculated the observed net enthalpy of reaction shown in Table 10. When these values are compared to the thermodynamic calculations, a constant enthalpy difference is seen for all temperatures above 25°C. This missing enthalpy can only be explained if the overall reaction is

(A)	$H_2 \rightarrow 2H_I$	slow, decreasing with higher temperatures
(B)	$H_2 \rightarrow 2H_{II}$	fast
(C)	$C_2H_4 + 2H_I \rightarrow C_2H_6$	fast
(D)	$C_2H_6 + 4H_{II} \rightarrow 2CH_4$	fast

in which the hydrogenation step involves only adsorbed hydrogen H_I and hydrogenolysis H_{II}. The rate of adsorption of H_I is so slow that it is not replenished during the passage of the pulse, thus its enthalpy of adsorption is missing from the overall energy balance. Presumably it is adsorbed in the interval (20 min) between pulses, but

TABLE 9
C_2H_4 IN H_2[a]

Temperature (°C)	Pulse no.	Observed heats (cal × 10^2)			Effluent gas (moles × 10^6)			
		exo	endo	exo	H_2	CH_4	C_2H_6	C_2H_4
23	1	20.0	—	—	—	tr	5.85	—
	2	19.6	—	—	—	tr	5.85	—
	3	19.1	—	—	—	0.04	5.83	—
	4	19.1	—	—	—	0.03	5.84	—
	5	20.0	—	—	—	0.01	5.85	—
150	1	—	1.09	—	—	tr	5.85	—
	2	—	1.04	—	—	0.02	5.84	—
	3	—	1.04	—	—	0.02	5.84	—
250	1	—	0.36	0.40	—	0.03	5.84	—
	2	—	0.26	0.60	—	0.03	5.84	—
	3	—	0.22	0.60	—	0.03	5.84	—
280	1	—	—	1.23	—	0.62	5.54	—
	2	—	—	1.23	—	0.62	5.54	—
300	1	4.17	—	—	—	4.82	3.43	—
	2	4.11	—	—	—	4.82	3.40	—
350	1	9.59	—	—	—	11.75	—	—
	2	9.59	—	—	—	11.75	—	—
	3	9.59	—	—	—	11.75	—	—

[a] Pulse Size: 5.85 × 10^{-6} g moles.

TABLE 10

Temperature (°C)	Net heat observed C_2H_4 (kcal/mole)	Net heat calculated C_2H_4 (kcal/mole)	Enthalpy difference C_2H_4 (kcal/mole)
23	−33.44	−32.74	
150	+ 1.82	−33.30	−35.12
250	− 0.43	−33.76	−33.33
280	− 2.10	−34.61	−32.51
300	− 7.08	−40.62	−33.54
350	−16.39	−50.58	−34.19

the resulting thermal peak is so broad that it is not detected. Type H_{II} is replaced immediately. At 25°C, the adsorption of H_I is fast enough so that other factors may become controlling. At higher temperatures, however, the formation of this mode may limit the rate in continuous operation.

What is the nature of type H_I and why does ethylene react only with this type. From the enthalpy deficiency, the enthalpy of H_I must be −34 kcal/mole, i.e., the most strongly held mode of hydrogen adsorption. Quantum mechanical calculations based on the localized bond theory (*15*) have identified this heat of adsorption with hydrogen held in the interstices of the (100) plane by five *d*-orbitals from surrounding nickel atoms. An ethylene molecule weakly adsorbed by a π-bond at one of the surface atoms would have the correct spatial arrangement to facilitate hydrogenation by these atoms. This would be the most favored mode for a fully covered surface since adsorption by two sites would require vacant nickel neighbors, a situation less likely. In the case of the experiment with preadsorbed hydrogen, however, many such sites are available, since only a small fraction of the total surface is covered. This type of adsorption may be hydrogenated by any available adsorbed hydrogen atom, perhaps in the step-wise mechanism suggested by many investigators.

The formation of type H_I is controlled by migration. Possibly adsorption occurs at other more accessible sites and is followed by transitions to the interstices. The rate of formation of H_I through this mechanism of migration will be dependent upon the coverage by adsorbed hydrogen. At the low coverages used in the hydrogen pulsing experiments, the rate of formation and the number is small. At the higher pressures in the ethylene hydrogenation studies, the coverage is high enough that, given sufficient time, a high concentration of type H_I is developed. This is evident since there is always sufficient H_I to hydrogenate completely the pulse of ethylene. At 25°C, the supply is replaced within the time of the passage of the pulse, while at higher temperatures this is not the case.

It is not clear why the rate of formation of H_I should decrease with temperature. Surface migration of adatoms is expected to increase with a temperature rise. If overall coverage decreases with increasing temperature and the rate of H_I formation is related to this coverage, then concentration of H_I might be expected to fall accordingly. Further investigation will be necessary before these factors are fully resolved.

In summary, when hydrogen coverage is low, there are sufficient sites for ethylene adsorption. Both hydrogen and ethylene adsorb only on the (100) planes. Hydrogenation to ethane proceeds either through (1) a reaction between molecular ethylene and an associatively adsorbed ethylene species which is just about to dissociate or (2) a reaction between adsorbed hydrogen and molecular or adsorbed ethylene. Path (2) is much faster than path (1). At higher temperature, ethylene also adsorbs and dissociates into methane and carbon.

With high hydrogen coverage, the ethylene does not adsorb strongly, but rather reacts via a π-adsorbed species with the interstitial adatoms of hydrogen in the (100) planes. The limiting step is the ad-

sorption and migration of hydrogen to these sites.

Thus different combinations of mechanisms will occur depending upon the hydrogen partial pressure and temperature. It has been demonstrated previously that nonequilibrium adsorption mechanisms of this type lead to the observed kinetics (*29*).

CONCLUSIONS

These experiments have demonstrated the usefulness of PTK studies in the study of surface catalysis. Features not otherwise detectable by more conventional means have been observed. The heats of adsorption of ethylene in different forms have been confirmed and many of the previous observations in the behavior of adsorbed ethylene substantiated quantitatively.

In addition, the reactions of ethylene with different types of adsorbed hydrogen have been demonstrated and new light shed on the nature of the surface mechanism so that it appears that the rate of adsorption of hydrogen to form the active species may be limiting.

REFERENCES

1. ELEY, D. D., *Catalysis* **3,** 49 (1955).
2. BOND, G. C., "Catalysis by Metals." Academic Press, New York, 1962.
3. RICHARDSON, J. T., FRIEDRICH, H., AND MCGILL, R. N., *J. Catal.* **37,** 1 (1975).
4. HORIUTI, J., *J. Res. Inst. Cat. Hokkaido Univ.* **6,** 250 (1958).
5. SELWOOD, P. W., "Adsorption and Collective Paramagnetism." Academic Press, New York, 1962.
6. HORIUTI, J., AND POLANGI, M., *Trans. Faraday Soc.* **30,** 1164 (1934).
7. JENKINS, G. I., AND RIDEAL, E. K., *J. Chem. Soc.* 2490 (1955).
8. TWIGG, G. H., *Disc. Faraday Soc.* **8,** 159 (1950).
9. ZUR STRASSEN, H., *Z. Physik. Chem.* **A169,** 81 (1934).
10. TAYLOR, T. I., *Catalysis* **5,** 257 (1957).
11. BOND, G. C., AND WELLS, P. B., *Advan. Catal.* **15,** 91 (1964).
12. EISCHENS, R. P., AND PLISKIN, W. A., *Advan. Catal.* **10,** 1 (1958).
13. SELWOOD, P. W., *J. Amer. Chem. Soc.* **83,** 2853 (1961).
14. MCKEE, D. W., *J. Amer. Chem. Soc.* **84,** 1109 (1962).
15. SHOPOV, D., ANDREEV, A., AND PETKOV, D., *J. Catal.* **13,** 123 (1969).
16. HORIUTI, J., AND TOYA, T., *Solid State Surface Sci.* **2,** 1 (1969).
17. SCHUIT, G. C. A., AND VAN REIJEN, L. L., *Advan. Catal.* **10,** 243 (1958).
18. COENEN, J. W. E., AND LINSEN, B. G., "Physical and Chemical Aspects of Adsorbents and Catalysts," p. 471. Academic Press, London, 1970.
19. MORIKAWA, K., SHIRASAKI, T., AND OKADA, M., *Advan. Catal.* **20,** 97 (1969).
20. BEECK, O., *Advan. Catal.* **2,** 151 (1950).
21. BOND, G. C., *Disc. Faraday Soc.* **41,** 200 (1966).
22. SHIGEHARA, Y., AND OZAKI, A., *J. Catal.* **15,** 224 (1969).
23. OZAKI, A., SHIGEHARA, Y., AND OGASAWARA, S., *J. Catal.* **8,** 22 (1967).
24. VAN HARDEVELD, R., AND HARLOG, F., *Surface Sci.* **15,** 189 (1969).
25. SCHNEIDER, P., AND SMITH, J. M., *AIChE J.* **14,** 763 (1968).
26. BROWNING, L. C., AND EMMETT, P. H., *J. Amer. Chem. Soc.* **74,** 1680 (1952).
27. BEECK, O., *Disc. Faraday Soc.* **8,** 118 (1950).
28. KOKES, R. J., AND BARTEK, J. P., *J. Catal.* **12,** 72 (1968).
29. HALSEY, G. D., *J. Phys. Chem.* **67,** 2038 (1963).